

## The Galileo Plasma Wave Investigation

D. A. GURNETT(1), W. S. KURTH(1), R. R. SHAW(+), A. ROUX(2), R. GENDRIN(2), C. F. KENNEL(3), F. L. SCARF(+), and S. D. SHAWHAN(+)

1 Department of Physics and Astronomy, The University of Iowa, Iowa City, IA 52242, U.S.A.

2 Centre National d'Etudes des Telecommunications/Centre de Recherches en Physique de l'Environnement Terrestre et

Planetaire, 92131 Issy-les-Moulineaux, Cedex, France.

3 Department of Physics, UCLA, Los Angeles, CA 90024, U.S.A.

+ Deceased

### Abstract.

The purpose of the Galileo plasma wave investigation is to study plasma waves and radio emissions in the magnetosphere of Jupiter. The plasma wave instrument uses an electric dipole antenna to detect electric fields, and two search coil magnetic antennas to detect magnetic fields. The frequency range covered is 5 Hz to 5.6 MHz for electric fields and 5 Hz to 160 kHz for magnetic fields. Low time-resolution survey spectrums are provided by three on-board spectrum analyzers. In the normal mode of operation the frequency resolution is about 10%, and the time resolution for a complete set of electric and magnetic field measurements is 37.33 s. High time-resolution spectrums are provided by a wideband receiver. The wideband receiver provides waveform measurements over bandwidths of 1, 10, and 80kHz. These measurements can be either transmitted to the ground in real time, or stored on the spacecraft tape recorder. On the ground the waveforms are Fourier transformed and displayed as frequency-time spectrograms. Compared to previous measurements at Jupiter this instrument has several new capabilities. These new capabilities include (1) both electric and magnetic field measurements to distinguish electrostatic and electromagnetic waves, (2) direction finding measurements to determine source locations, and (3) increased bandwidth for the wideband measurements.

### 1. Introduction

This paper describes the Galileo plasma wave investigation. The basic objective of this investigation is the study of plasma waves and radio emissions in the magnetosphere of Jupiter. The Voyager 1 and 2 flybys of Jupiter have now clearly shown that many complex types of plasma wave and radio emission phenomena occur in the Jovian magnetosphere (Scarf et al., 1979; Warwick et al., 1979a, b; Gurnett et al., 1979). These include electromagnetic whistler mode emissions called chorus and hiss, continuum radiation trapped in the magnetospheric cavity, electrostatic waves associated with harmonics of the electron cyclotron frequency, electrostatic and electromagnetic ion-cyclotron waves, and a wide variety of escaping radio

emissions. Some of these waves, such as the whistler mode emissions and ion cyclotron waves, are believed to play an important role in the dynamics of the magnetosphere by controlling the pitch-angle scattering and loss of magnetically trapped radiation belt particles. Certain types of plasma waves, such as lightning generated whistlers and upper hybrid resonance emissions, provide important diagnostic tools, from which fundamental plasma parameters such as the electron density can be computed. For an overview of plasma waves in the Jovian magnetosphere see, for example, the review by Gurnett and Scarf (1983).

Since the Galileo spacecraft will be the first orbiter of Jupiter, this spacecraft will provide much better spatial coverage of the Jovian magnetosphere than was possible with the previous Pioneer and Voyager flybys of Jupiter. Specifically, the orbit of Galileo will provide a survey of the magnetotail near local midnight at distances of up to 150 R<sub>J</sub>, a region that has never previously been explored; repeated passes through the plasma sheet, the magnetopause, and the tail lobes; and numerous close flybys of the Galilean satellites. Of particular importance will be a very close pass by the satellite Io. The Voyager flybys showed that volcanic gases escaping from Io are the main source of plasma in the Jovian magnetosphere and that the primary energization occurs in the dense torus of plasma that surrounds Jupiter near Io's orbit.

In addition to exploring regions never previously investigated, Galileo, by virtue of its long lifetime in orbit around Jupiter, also provides a unique new capability for carrying out studies of temporal variations on time scales that cannot be investigated with a single flyby. For example, it is known that the kilometric and decametric radio emissions associated with Io and its plasma torus have temporal variations on time scales of weeks and longer. With Galileo these temporal variations can be monitored over periods of several years and compared with other remote sensing instruments. These measurements should be able to tell us, for example, whether the variations are associated with volcanic eruptions on Io or some other cause. Considerable interest also exists in searching for evidence of magnetospheric substorm phenomena, possibly comparable to auroral substorms in the Earth's magnetosphere (Akasofu, 1976). With the Galileo plasma wave instrument, it should be possible to provide remote sensing of substorms in a manner comparable to the remote sensing of terrestrial auroral kilometric radiation, which is known to be closely associated with terrestrial substorms. Remote detection of lightning, from whistler measurements, can also provide information on convective storms in Jupiter's atmosphere.

To carry out comprehensive studies of plasma waves and radio emissions at Jupiter, the Galileo plasma wave instrument incorporates several new features that provide improvements over the previous Voyager 1 and 2 measurements. These improvements include (1) both electric and magnetic field measurements to distinguish electrostatic waves from electromagnetic waves, (2) direction finding measurements to determine source locations, and (3) wideband measurements with increased bandwidth to resolve fine structure in the plasma wave and radio emission spectrum. The main instrument package and the electric antenna system were designed and constructed at the University of Iowa, and the search coil magnetic antenna was provided by the Centre de Recherches en Physique de l'Environnement Terrestre et Planetaire (CRPE). A summary of the principal instrument characteristics is given in Table I and a detailed description of the instrument is given in Sections 2 and 3. Section 4 describes the instrument calibration and Section 5 describes the in-flight performance.

TABLE I  
Plasma wave instrument characteristics

	Characteristic
Frequency range, electric	5.62 Hz to 5.65 MHz
Frequency range, magnetic	5.62 Hz to 160 kHz
Frequency resolution 67%	(Low freq.) 5.62 Hz to 31.1 Hz, DELTA f/f ~
8%	(Med. freq.) 40 Hz to 160 kHz, DELTA f/f ~
~ 10%	(High freq.) 100 kHz to 5.65 MHz, DELTA f/f
Time resolution 2.67 s	(Low freq.) 5.62 Hz to 31.1 Hz, DELTA t =
18.67 s	(Med. freq.) 40 Hz to 160 kHz, DELTA t =
18.67 s	(High freq.) 100 kHz to 5.65 MHz, DELTA t =
Sensitivity, electric	$E/\sqrt{\text{DELTA } f} \sim 15 \text{ nV m}^{-1} \text{ Hz}^{-1/2}$ at 10 kHz
Sensitivity, magnetic Hz	$B/\sqrt{\text{DELTA } f} \sim 50 \mu \text{ gamma Hz}^{-1/2}$ at ~ 100 decreasing to ~ 3 $\mu \text{ gamma Hz}^{-1/2}$ at 20 kHz
Dynamic range	5.62 Hz to 31.1 Hz, 110 db 40 Hz to 5.65 MHz, 100 db
Wideband waveform modes	Mode 1, 50 Hz to 10 kHz Mode 2, 50 Hz to 80 kHz Mode 3, 5 Hz to 1 kHz
Waveform resolution	Mode 1, 4-bits, 25 200 samples $s^{-1}$ Mode 2, 4-bits, 201 600 samples $s^{-1}$ Mode 3, 4-bits, 3150 samples $s^{-1}$
Mass	Main electronics box 3.94 kg Search coil 1.52 Electric antenna 1.68 ----- Total 7.14 kg
Power	6.80 W, heater power 3.0 W

## 2. Electric and Magnetic Field Sensors

The plasma wave sensors on Galileo consist of one 6.6 m tip-to-tip electric dipole antenna and two search coil magnetic antennas. The electric dipole antenna is mounted at the end of the magnetometer boom approximately 10.6 m from the spacecraft, as shown in Figure 1, and the search coil magnetic antennas are mounted on the high gain antenna feed. The electric antenna consists of two graphite epoxy elements with a root diameter of 2.0 cm, tapering to a diameter of 0.3 cm at the tip. To minimize electric field asymmetries induced by the spacecraft structure the dipole elements are mounted perpendicular to the magnetometer boom. The antenna axis is also oriented perpendicular to the spacecraft spin axis in order to permit direction finding. Each element is hinged 1.8 m from the tip so that the antenna can be folded for launch. A housing at the base of the dipole elements contains two pre-amplifiers. These pre-amplifiers provide low impedance signals to the main electronics package, one for each element. Each element is grounded to the spacecraft structure through a 250 mega-ohm resistance to limit differential charging effects. A photograph of the electric antenna assembly is shown in Figure 2.

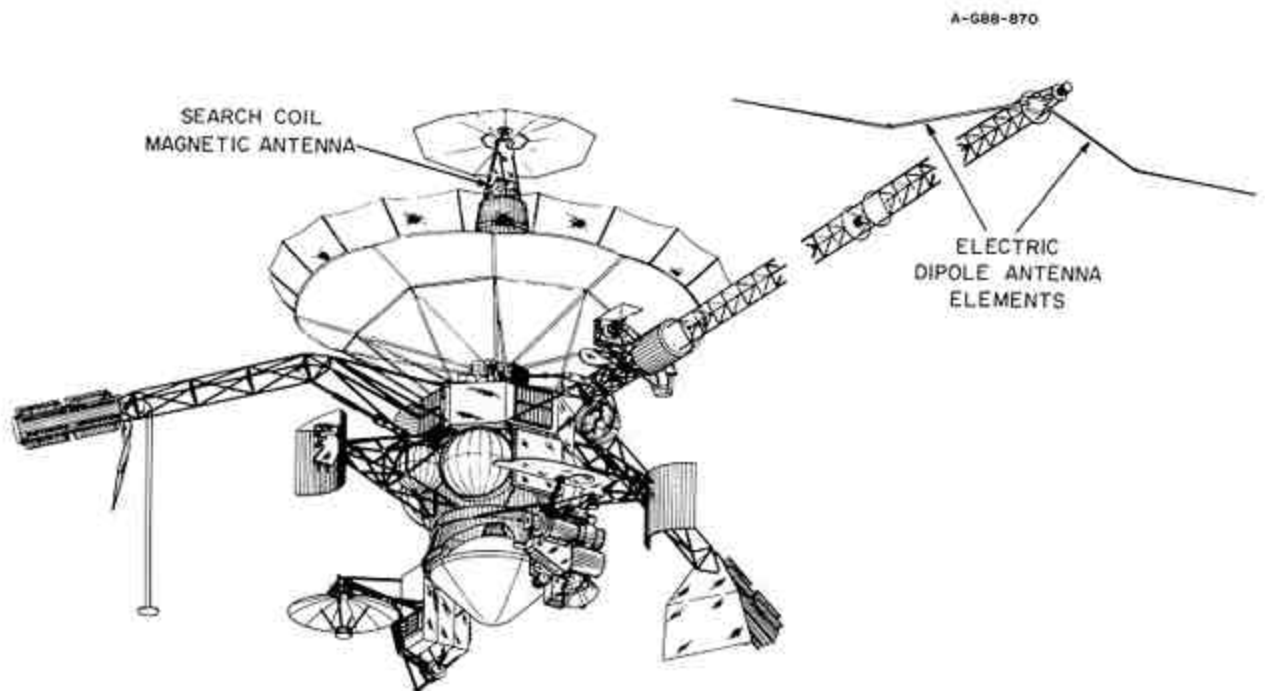


Fig. 1. A sketch of the Galileo spacecraft showing the location and orientation of the electric dipole and search coil antennas used by the plasma wave instrument.

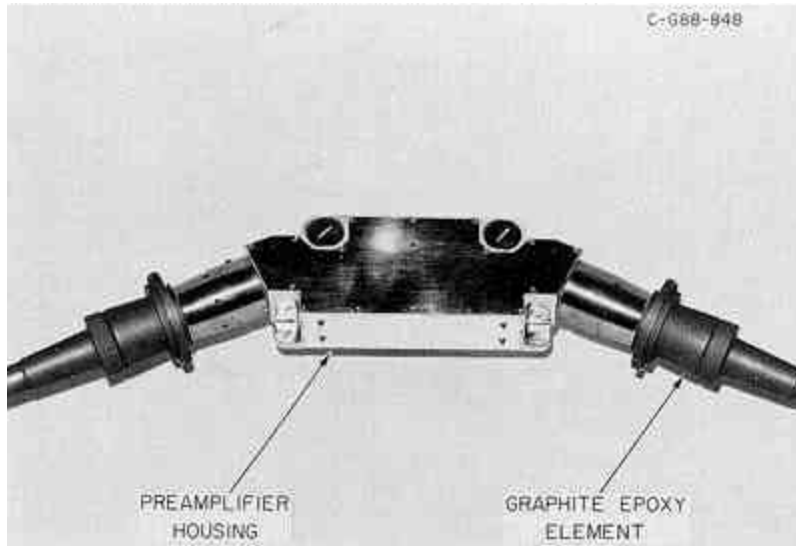


Fig. 2. A photograph of the electric dipole antenna and preamplifier assembly. This assembly is mounted on the end of the magnetometer boom as shown in Figure 1.

The search coil magnetic antenna consists of two high permeability rods, 25.5 and 27.5 cm long, one optimized for low frequencies, 5 Hz to 3.5 kHz, and the other optimized for high frequencies, 1 to 50 kHz. The winding on the low frequency search coil consists of 50000 turns of 0.07 mm diameter copper wire and the winding on the high-frequency search coil consists of 2000 turns of 0.14 mm diameter copper wire. The two search coils are mounted orthogonally to minimize the electrical coupling between the sensors. Both search coils are mounted perpendicular to the spacecraft spin axis. The high-frequency sensor is oriented perpendicular to the electric dipole antenna and the low-frequency sensor is oriented parallel to the electric dipole antenna. Two preamplifiers are mounted in a housing near the search coils in order to provide low impedance signals to the main electronics package. Photographs of the search coil and pre-amplifier assemblies are shown in Figure 3.

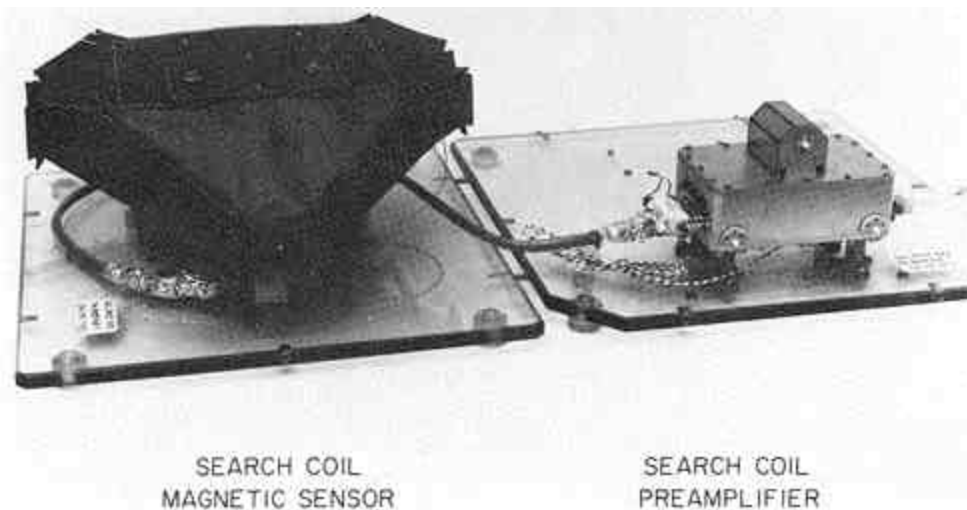


Fig. 3. A photograph of the search coil magnetic sensor assembly. These assemblies are mounted on the high gain antenna as shown in Figure 1.



Fig. 4. A photograph of the main electronics housing. This housing is mounted in the spacecraft body near the base of the magnetometer boom.

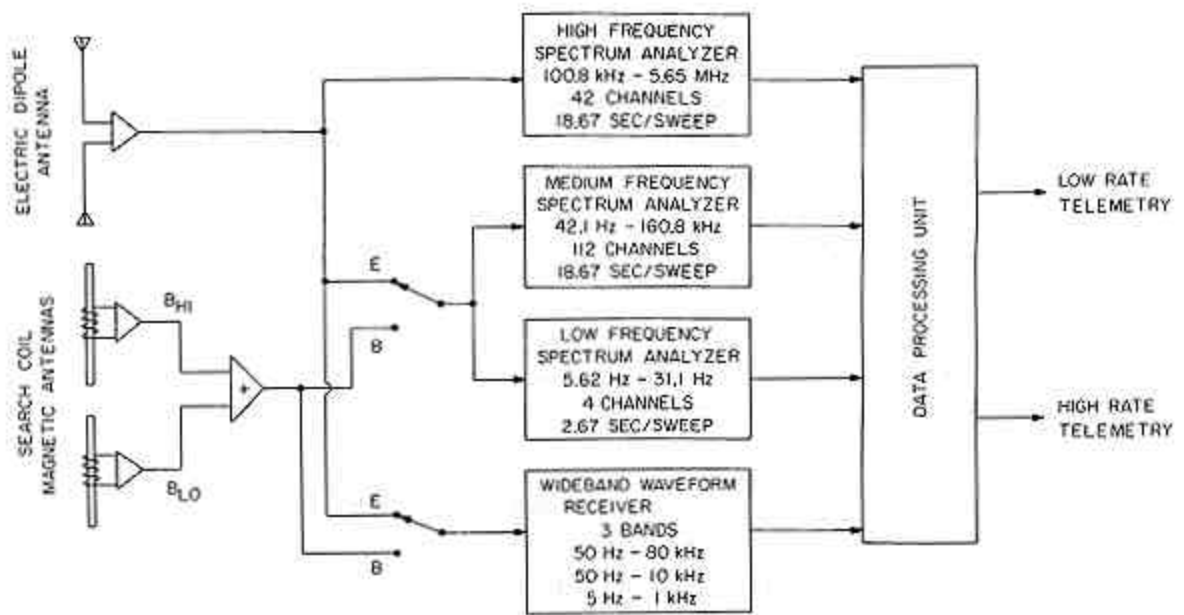


Fig. 5. A block diagram of the plasma wave instrument electronics. Signals from the electric and magnetic antennas are processed by three spectrum analyzers (at low, medium, and high frequencies) and a wideband waveform receiver. All analog to digital conversions and instrument control functions are handled by a data processing unit which interfaces with the spacecraft Command and Data System (CDS).

### 3. Main Electronics Package

All of the signal processing for the plasma wave experiment is performed in a single main electronics package. The main electronics package is mounted in the spacecraft body near the base of the magnetometer boom. A photograph of the main instrument housing is shown in Figure 4, and a simplified block diagram of the instrument is shown in Figure 5. The signal processing is performed by two main systems, a low rate system to provide survey spectrums, and a high rate system to provide high resolution (wideband) spectrums. The low rate system consists of three spectrum analyzers: a high-frequency spectrum analyzer, a medium-frequency spectrum analyzer, and a low-frequency spectrum analyzer. The high-frequency spectrum analyzer provides 42 frequencies from 100.8 kHz to 5.645 MHz with a fractional frequency spacing of  $\Delta f/f \sim 10.0\%$  and a band-width of 1.34 kHz. The dynamic range of the high-frequency analyzer is 100 db, and a complete spectral sweep requires 28 minor telemetry frames, which corresponds to 18.67 s. The medium-frequency spectrum analyzer provides 112 frequencies from 40 Hz to 160 kHz with a fractional frequency spacing of  $\Delta f/f \sim 8.0\%$ . The 112 frequencies of this analyzer are divided into four bands, each with 28 frequencies. The filter bandwidths associated with each of these bands (in order of increasing frequency) are 4.26, 6.67, 120, and 1510 Hz. The medium-frequency analyzer gives one spectral sweep every 18.67 s with a dynamic range of 100 db. The low-frequency analyzer provides 4 logarithmically-spaced frequency channels from 5.62 to 31.1 Hz with filter bandwidths of 0.83, 1.86, 2.75, and 4.79 Hz. These 4 channels are sampled once every 2.67 s and have a dynamic range of 110 db. The exact sampling scheme for the high-, medium-, and low-frequency spectrum analyzers is somewhat complex and is summarized in Figure 6. As can be seen the basic cycle time required to obtain a complete spectrum from one antenna is 18.67 s. The signals from the spectrum analyzer filters are logarithmically compressed and detected using a circuit that provides a piecewise-linear approximation to a logarithmic response. The outputs from the logarithmic compressors are then digitized with 8-bit resolution and transmitted to the ground via the low rate telemetry system. The effective data rate for the low rate portion of the instrument is 240 bits  $s^{-1}$ .

The high rate wideband receiver provides waveform measurements in three frequency bands, 5 Hz to 1 kHz, 50 Hz to 10 kHz, and 50 Hz to 80 kHz. The frequency band used is controlled by signals from the spacecraft Command and Data Subsystem (CDS). Waveforms from the wideband receiver are digitized by a 4-bit analog to digital converter. Since 4-bit digitization only provides a dynamic range of about 24 db, an analog automatic gain control (AGC) circuit is used to control the amplitude of the waveforms into the analog to digital converter. The AGC time constant is 0.1 s in the two high frequency bands and 1.0 s in the low-frequency band. The sample rate is either

3150, 25 200, or 201 600 samples per second, depending on the frequency band selected. The waveform data can be either transmitted in real time or recorded on the spacecraft digital tape recorder.

The plasma wave instrument has several modes of operation and methods of data transmission. These modes are also controlled by the spacecraft CDS. The medium and low-frequency spectrum analyzers and the wideband waveform receiver can be connected to either the electric dipole antenna or the search coil magnetic antennas. In the normal mode of operation, the medium- and low-frequency spectrum analyzers are cycled between the electric and magnetic antennas so that alternate electric and magnetic spectrums are obtained. Since the search coils do not provide signals in the frequency range covered by the high-frequency analyzer, this analyzer is always connected to the electric antenna. In the cycling mode of operation, the time required for a complete set of electric and magnetic field spectrums is 37.33 s. The medium- and low-frequency analyzers can also be locked on either the electric or magnetic antennas to provide improved time resolution at the expense of complementary electric and magnetic field coverage. In the ground data processing the spectrum analyzer data are displayed in the form of color frequency-time spectrograms. The frequency scale of the Galileo spectrograms extends from 5.6 Hz to 5.65 MHz, and variable time scales are available, ranging from 30 min to more than 24 hours, depending on the application. Normally, 24-hour spectrograms are used for the low rate survey data. These survey spectrograms are used to select specific intervals for more detailed analysis, such as comparison with charged particle or magnetic field data, or direction-finding analyses.

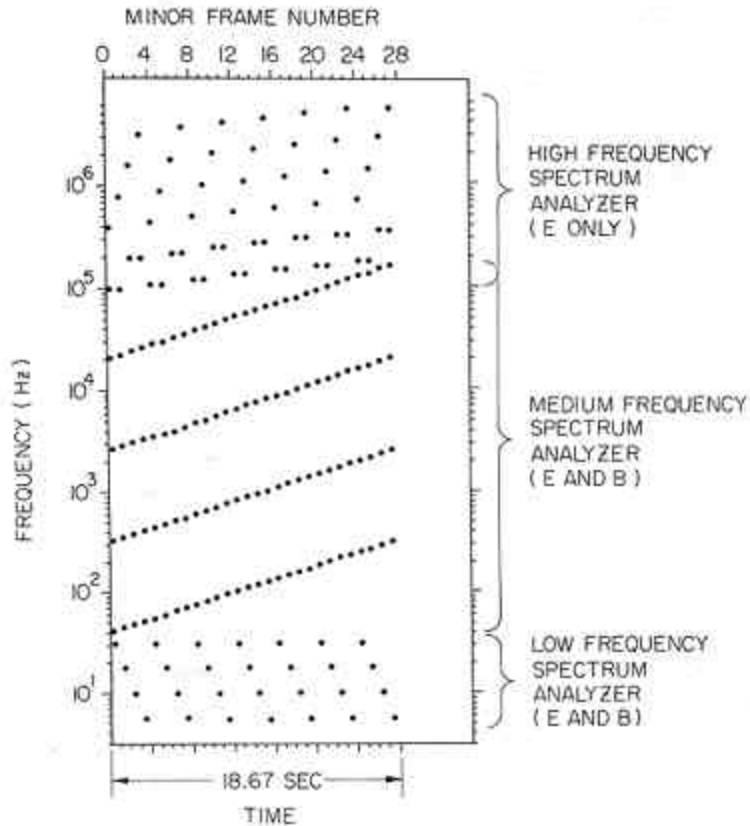


Fig. 6. A diagram showing the scheme for sampling the outputs from the various receiver channels. The basic sampling cycle requires 28 minor frames, which corresponds to 18.67 s.

TABLE II  
Representative Hi-rate waveform modes

Spacecraft of mode block	Time interval between data blocks	Instrument Duty Hi-rate mode cycle	Frequency coverage	Frequency resolution	Size data
MPW bits (R/T or record)	66 2/3 ms	Mode 3 61% (12.6 kb s <sup>-1</sup> )	5 Hz-1 kHz	25 Hz  (64 freq.)	512
MPP bits (R/T or record)	66 2/3 ms	Mode 3 100% (12.6 kb s <sup>-1</sup> )	5 Hz-1 kHz	any desired resolution	840

H CJ, H P J bits 66 2/3 ms (R/T)	Mode 3 100% (12.6 kb s <sup>-1</sup> )	5 Hz-1 kHz	any desired resolution	840
X P W, X R W bits 66 2/3 ms (R/T)	Mode 1 46% (100.8 kb s <sup>-1</sup> )	50 Hz-10 kHz	49 Hz (256 freq.)	3104
H P W, H R W bits 66 2/3 ms (R/T or record)	Mode 1 94% (100.8 kb s <sup>-1</sup> )	50 Hz-10 kHz	25 Hz (512 freq.)	6304
P W 4 bits 8 1/3 ms (Record)	Mode 2 46% (806.4 kb s <sup>-1</sup> )	50 Hz-80 kHz	394 Hz (256 freq.)	3104
P W 8 bits 8 1/3 ms (Record)	Mode 2 95% (806.4 kb s <sup>-1</sup> )	50 Hz-80 kHz	197 Hz (512 freq.)	6400
W F Survey bits 18 2/3 s	Mode 4 - (in LRS data) and	50 Hz-10 kHz 5 Hz-1 kHz	98 Hz 12 Hz (128 freq.)	1120

-----  
-----  
^a Based on using FFT techniques on 1 block of data only.

The greatest flexibility in the operation of the plasma wave instrument is available in the wideband waveform receiver. This receiver provides very high-resolution measurements of electric and magnetic field waveforms during times of special interest, such as the pass through the Io torus and satellite encounters. The waveform data provide the highest possible frequency and time resolution, subject only to the constraints of Fourier analysis,  $\Delta f \Delta t \sim 1$ . Although the waveform receiver has only three frequency bands, with bit rates of 12.6, 100.8, and 806.4 kbits/sec, several spacecraft modes are available for recording and transmitting the data to the ground. These modes of wideband data transmission and the corresponding time resolution for the most conveniently usable "blocks" of wideband data are summarized in Table II. In the highest time resolution mode, a continuous sample of the electric or magnetic field waveform can be obtained over a bandwidth of 50 Hz to 80 kHz for periods of up to 18 min (the time required to fill the spacecraft tape recorder).

On the ground the waveform data are Fourier transformed in discrete packets, usually consisting of 1024 samples, and displayed in the form of a frequency-time spectrogram. These frequency-time spectrograms provide the highest time resolution data available from the Galileo plasma wave instrument. In certain modes of operation, such as MPW, XPW, and PW4, the duration of the wideband recording can be extended at the expense of reduced duty cycle, frequency coverage, or analysis bandwidth. To provide waveform

measurements when the high rate telemetry link is not available, a waveform survey output is included in the regular low rate telemetry data. This waveform survey output provides one block of 280 waveform samples every 18.67 s in any of the three wideband frequency ranges, 5 Hz to 1 kHz, 50 Hz to 10 kHz, or 50 Hz to 80 kHz.

#### 4. Instrument Calibration

An extensive series of calibrations and performance checks were carried out on the plasma wave instrument both before and after integration on the spacecraft. Since the piecewise-linear logarithmic compressors used in the spectrum analyzers do not give a true logarithmic response, the transfer function of the logarithmic compressors must be calibrated. Since a large number of channels are used, it was not practical to measure the transfer function for each frequency channel separately. Since the receivers are organized into distinct frequency bands, each of which uses the same filter and logarithmic compressor, the calibration can be broken into two steps. First, within a given band the transfer function from antenna input to the telemetry output is measured by progressively increasing the signal amplitude at a fixed frequency. Second, within this same band the frequency response is measured, from channel to channel, at a fixed input amplitude. By combining these amplitude and frequency response measurements a complete calibration can be obtained for all signal intensities and frequencies.

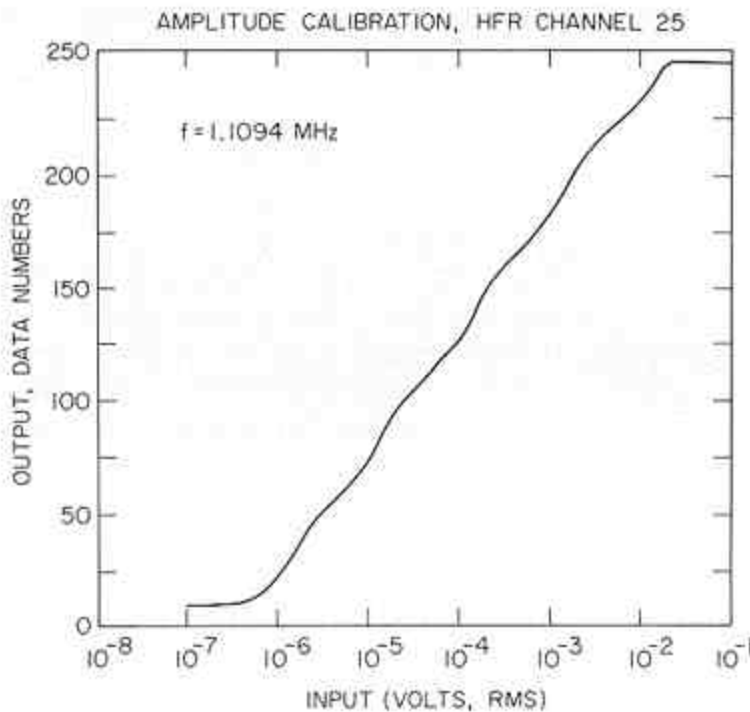


Fig. 7. A representative transfer function for a single channel of the high-frequency spectrum analyzer. The deviation from a straight line is caused by the piecewise-linear stages in the logarithmic compressor.

A representative transfer function is shown in Figure 7. This curve is for channel 25 (1.1094 MHz) of the high-frequency receiver. This transfer function gives the amplitude response of the logarithmic compressor, including all gain factors from the antenna (electric, in this case) to the logarithmic compressor. The slight deviation from a true logarithmic response is caused by the piecewise-linear response of the logarithmic compressor. Using calibration curves such as this, a look-up table can be constructed which converts the telemetry data number to input signal strength. When combined with the channel-to-channel gain, these calibrations are sufficient to determine the signal strength in all channels of the high-frequency receiver.

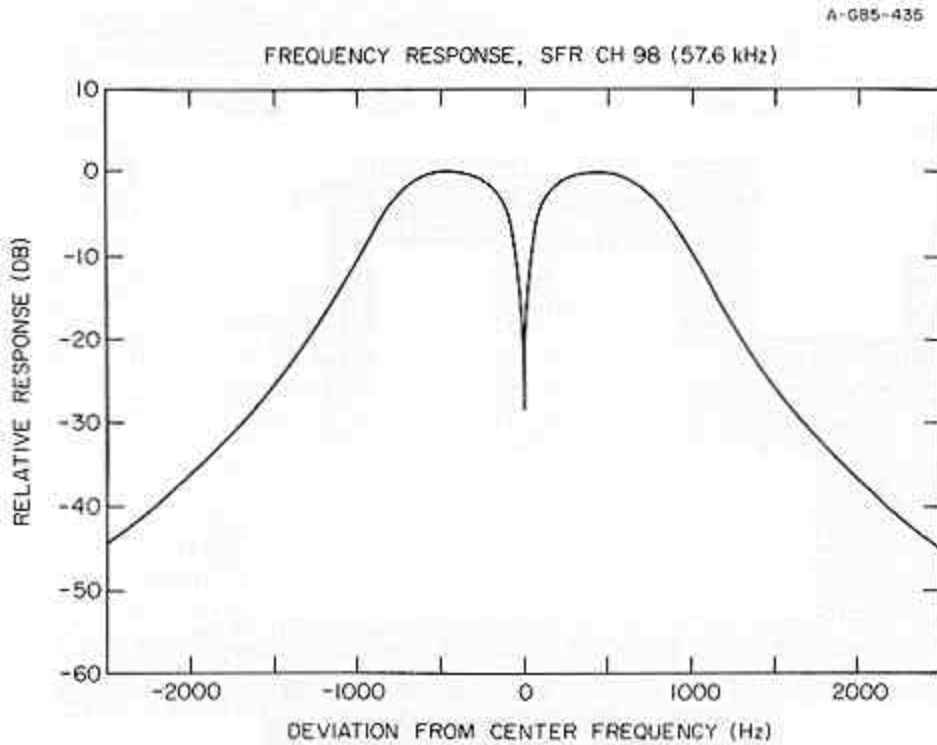


Fig. 8. A representative frequency response of a single channel of the medium frequency spectrum analyzer. The notch at the center of the band is caused by the frequency mixing scheme, which has the intermediate frequency (IF) at zero frequency.

In addition to measuring the transfer function and channel-to-channel gain, a detailed frequency response measurement was also performed for each filter. These measurements confirm that the filters have the proper shape and no spurious responses. A typical filter frequency response is shown in Figure 8. This frequency response curve is for channel 98 (57.6 kHz) of the medium-frequency spectrum analyzer. The sharp notch at the center of the filter band is characteristic of the type of receiver used (zero frequency IF). Whenever possible the notch is centered on harmonics of the spacecraft 2.4 kHz power supply in order to reduce spacecraft generated interference. The filter frequency response measurements provide a good first-order estimate of the noise bandwidth of the filters.

The effective noise bandwidths are also independently determined by stimulating the instrument with a white noise signal of known spectral density.

As can be seen from the transfer function curve in Figure 7, a level exists below which no signal can be detected. For our purposes the noise level of the instrument is defined as the signal level which gives a unity signal to noise ratio ( $S/N = 1$ ). Plots showing the noise levels for the electric and magnetic antennas are shown in Figures 9 and 10. These noise levels have been converted to units of electric and magnetic spectral densities. For the electric field antenna, the electric field strength is computed by assuming that the antenna has an effective length of  $l_{\text{eff}} = 3.5$  m. This length is the distance between the geometric centers of the two dipole elements. The discontinuities between various parts of the curve are due to differences in the internal noise levels of the high-, medium-, and low-frequency spectrum analyzers. For the search coil magnetic antennas, the magnetic field sensitivity and frequency response were calibrated in the IPG magnetic field observatory at Chambon La Foret, France. The transfer function measurements were performed using a Helmholtz coil driven by a known AC current source. The absolute accuracy of the magnetic field calibration is estimated to be about 3%. The magnetic noise levels were measured by placing the search coils in a mu-metal chamber, which shields the sensors from external noise sources.

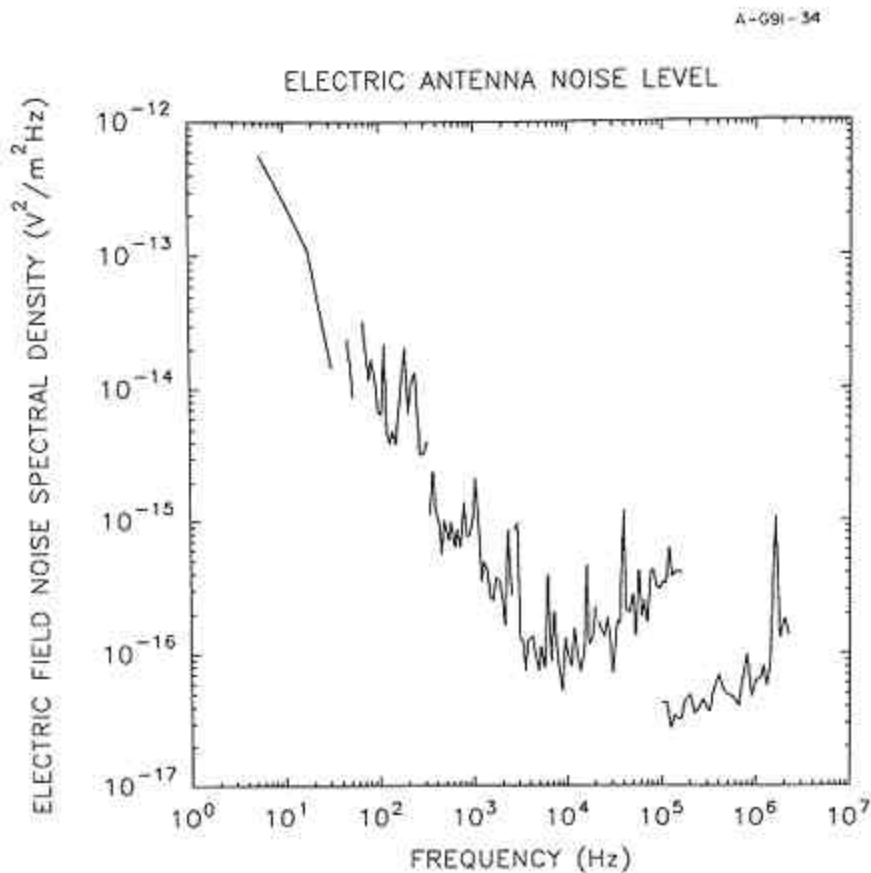


Fig. 9. The system level (unity signal-to-noise ratio) for the electric antenna system

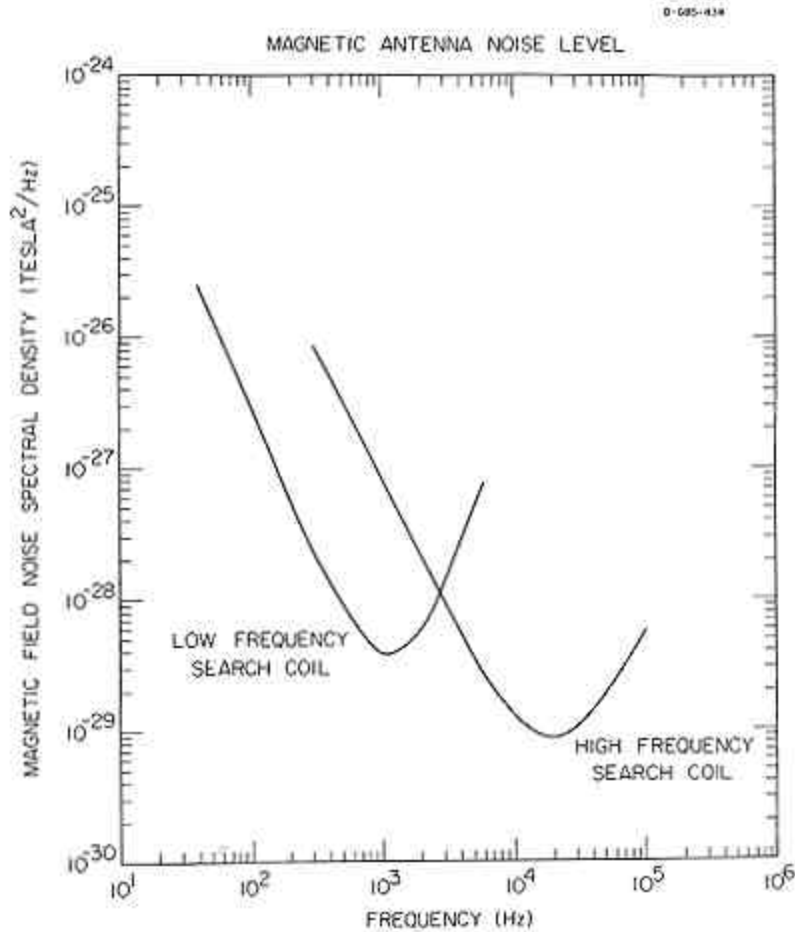


Fig. 10. The system level (unity signal-to-noise ratio) for the magnetic antenna system.

## 5. Inflight Performance.

The Galileo spacecraft was successfully launched on October 18, 1989. The plasma wave instrument was turned on shortly after launch and operated satisfactorily. During a period known as the '4-day checkout', which occurred from December 27 to 31, 1989, a detailed checkout of the instrument was performed, including tests to determine if any interference was present from other spacecraft systems or instruments. The instrument operation proved to be nominal in all respects. The electric field interference levels also proved to be very low. Only a few very minor interference lines could be detected, mostly in the high-frequency receiver channels. Many type III solar radio burst were detected during the 4-day checkout, which demonstrates the excellent sensitivity of the instrument. A frequency-time spectrogram showing some of these radio bursts is shown in Figure 11. A persistent elevation of the electric field noise levels above the pre-launch noise levels exists in the low-frequency channels, below about 100 Hz. This noise is essentially structureless, and appears to be caused by the plasma.

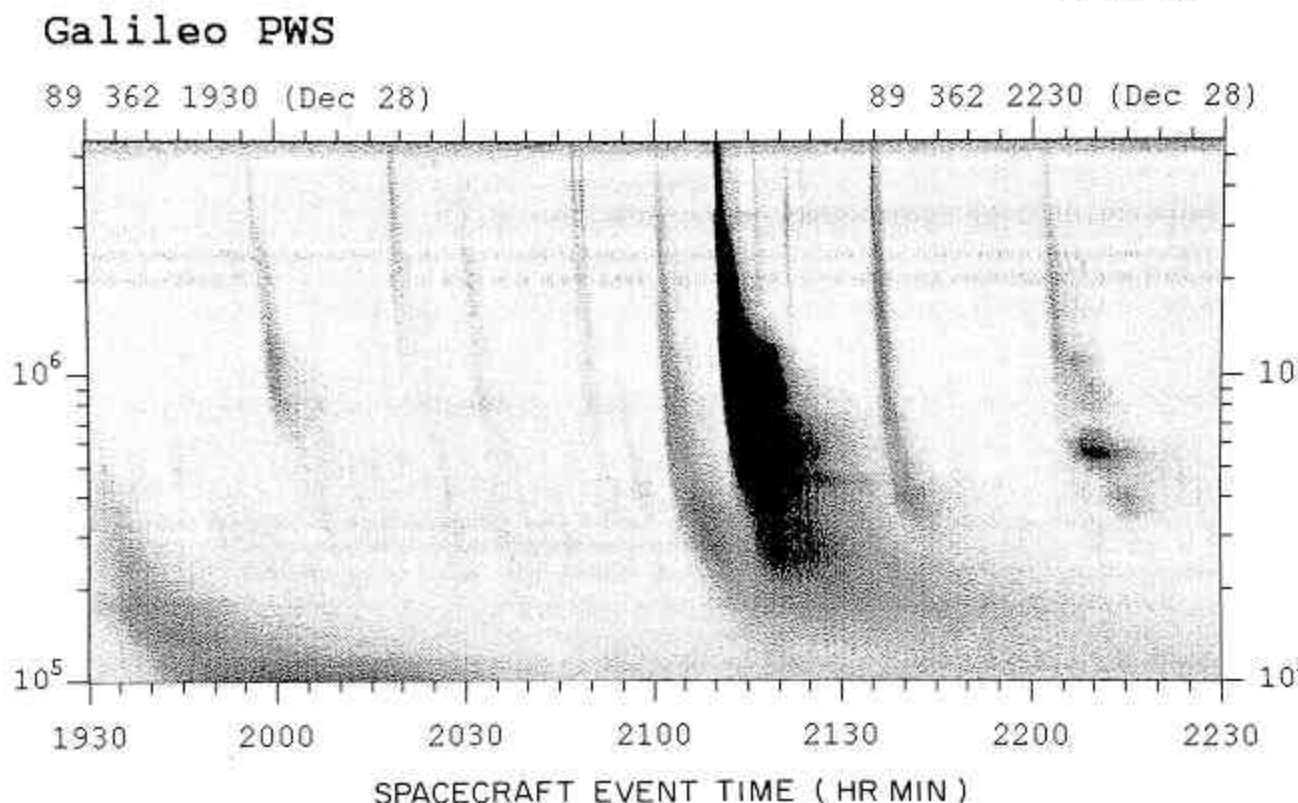


Fig. 11. A spectrogram showing numerous type III solar radio bursts detected during the 4-day checkout. Note the almost complete absence of spacecraft generated interference.

The magnetic field data showed a series of strong interference lines at the fundamental and low order harmonics of the 2.4 kHz spacecraft power supply. These magnetic interference lines extend as much as 20 db above the search coil noise level, and were comparable to the magnetic interference levels observed in the pre-launch testing. The strong magnetic interference is a consequence of the close proximity of the search coils to the spacecraft body, which has substantial power system currents at 2.4 kHz and its harmonics. It would have been much better to have mounted the search coil on a boom far from the spacecraft body. This option was considered early in the spacecraft design, but was rejected because of certain critical spacecraft weight and balance considerations which were of importance at that stage of the project. Although the power supply interference is undesirable, adequate measurements can still be made at frequencies between the harmonics. Therefore, the objectives of the magnetic field sensors are not seriously compromised. Strong interference was also detected from the ultraviolet spectrometer (UVS) at frequencies up to a few hundred Hz. This interference apparently originates from an unshielded stepper motor that was not identified as an interference source during the pre-launch testing. From a second compatibility test conducted during the Earth 1 flyby we demonstrated that the scientific impact of this interference can be minimized by duty cycle operation of the UVS instrument.

## 6. Conclusion

The Galileo plasma wave experiment is a capable instrument which should provide valuable new information on wave-particle interactions in the Jovian magnetosphere. The electric field noise levels are comparable to the Voyager plasma wave instrument and the magnetic field noise levels are comparable to those used on previous terrestrial plasma wave investigations. The frequency resolution is substantially better than the previous Voyager measurements, and the direction-finding and magnetic field measurements will provide an entirely new capability for measuring plasma waves and radio emissions in the Jovian magnetosphere.

## Acknowledgements

The authors would like to express their thanks to Steve Remington, Don Kirchner, Bob Barrie, Elwood Kruse, and Dave Tomash at the University of Iowa, for their role in designing, assembling, and testing the instrument; to Alain Meyer of CRPE for his role in designing the search coil magnetic antennas; to Terry Averkamp, Larry Granroth and Scott Allendorf of the University of Iowa and Claude de Villedary of CRPE for their role in preparing the data processing routines; and to Gaylon McSmith and Bill Fawcett at the Jet Propulsion Laboratory for their help in coordinating our effort with JPL. Unfortunately three of our co-investigators, Fred Scarf from TRW, Bob Shaw from the University of Iowa, and Stan Shawhan from NASA Headquarters have died during the course of this investigation. This instrument was funded by NASA through the Jet Propulsion Laboratory under contracts 955234 and 958779.

## References

- Akasofu, S.-I 1976, *Physics of Magnetospheric Substorms*, D. Reidel Publ. Co., Dordrecht, Holland.
- Gurnett, D. A. and Scarf, F. L.: 1983, in A. J. Dessler (ed.), 'Plasma Waves in the Jovian Magnetosphere', *Physics of the Jovian Magnetosphere*, Cambridge University Press, Cambridge, pp. 285-316.
- Gurnett, D. A., Kurth, W. S., and Scarf, F. L.: 1979, 'Plasma Wave Observations Near Jupiter: Initial Results from Voyager 2', *Science* 206, 987.
- Scarf, F. L. and Gurnett, D. A.: 1977, 'A Plasma Wave Investigation for the Voyager Mission', *Space Sci. Rev.* 21, 287.
- Scarf, F. L., Gurnett, D. A., and Kurth, W. S. : 1979, 'Jupiter Plasma Wave Observations: An Initial Voyager 1 Overview', *Science* 204, 991.
- Warwick, J. W., Pearce, J. B., Riddle, A. C., Alexander, J. K., Desch, M. D., Kaiser, M. L., Thieman, J. R., Carr, T. D., Gulkis, S., Boischoat, A., Harvey, C. C., and Pedersen, B.

M.: 1979a, 'Voyager 1 Planetary Radio Astronomy Observations Near Jupiter', *Science* 204, 995.

Warwick, J. W., Pearce, J. B., Riddle, A. C., Alexander, J. K., Desch, M. D., Kaiser, M. L., Thieman, J. R., Carr, T. D., Gulkis, S., Leblanc, Y., Pedersen, B. M., and Staelin, D. H.: 1979b, 'Planetary Radio Observations from Voyager 2 Near Jupiter', *Science* 206, 991.